Soft Matter

PAPER

View Article Online
View Journal | View Issue

Cite this: *Soft Matter*, 2026, **22**, 1008

Nonequilibrium surfactant partitioning into microdroplets generates local phase inversion conditions and interfacial instability

Samuel G. Birrer, [a] Sanjana Krishna Mani, [a] Bryan Kaehr, [b] Ayusman Sen [ac] and Lauren D. Zarzar *[ade]

Droplets far from equilibrium experience different compositions and local environments compared with bulk oil and water phases at equilibrium. Understanding the pathways involved in emulsion progression towards equilibrium is valuable for designing complex fluids for many purposes including coatings, food, chemical separations, active matter, and enhanced oil recovery. Here we report how microscale oil droplets, which partition nonionic surfactants and also solubilize, can follow an unexpected pathway wherein a spherical droplet transitions through an interfacial instability and dissociates. This process depends on the oil hydrophobicity, the concentration and ethylene oxide number of the surfactant, the initial droplet diameter, and the presence of neighboring droplets. We propose a mechanism based on local phase inversion that explains both the visual appearance of the droplet dissociation behavior as well as the trends in its counterintuitive dependence on specific conditions like oil and surfactant chemical structure and surfactant concentration.

Received 17th October 2025,
Accepted 5th January 2026

DOI: 10.1039/d5sm01049g

rsc.li/soft-matter-journal

Introduction

Out-of-equilibrium multiphase systems like emulsions are commonplace materials, and elucidating how such systems proceed towards equilibrium is useful for formulating, tailoring, and controlling their time-dependent physical properties. Emulsions are dispersions in which at least one liquid, the dispersed phase, is distributed as droplets within another immiscible liquid, the continuous phase. The kinetic stability of emulsions can be tuned using surfactants, but over a range of timescales, the droplets destabilize by various pathways such as Ostwald ripening, coalescence, dissolution, and solubilization.[1–3] Extensive research has addressed equilibrium conditions, such as surfactant molecule partitioning between bulk oil and water phases[4–6] or solubilization capacity (the maximum quantity of a substance that can be solubilized in a micellar solution).[2,7] However, understanding the kinetics of, and relationships between, the various non-equilibrium molecular transport pathways in emulsions has been more challenging.[8–13] Certain kinetic parameters, such as the interfacial mass transport coefficient (mass of oil solubilized per interfacial area per second), and investigation of the different pathways by which solubilization can occur, have been the subject of interest over decades.[2,7,10,14] Reminiscent of biological systems, many fascinating microscale, non-equilibrium physical phenomena can emerge as a result of the interactions between the different pathways. For example, solubilization (*i.e.* the transfer of droplet contents into the continuous phase surfactant micelles) can generate gradients that induce Marangoni flows and drive droplets to self-propel,[11,13,15] attract,[12] repel,[16] chase,[17] or collectively organize.[17–19] Bringing together two out-of-equilibrium phases of proper formulation can give rise to spontaneous emulsification, wherein droplets form without the input of additional energy.[20–23] Surfactant partitioning into non-equilibrium droplets can also occur[24] and give rise to non-intuitive outcomes such as changing contact angles of sessile oil droplets,[25] phase separations inside droplets,[24] genesis of new phases near the drop interface,[24] and decreasing interfacial tension over hours-long timescales.[24] Understanding the dynamic processes involved in determining the paths that droplets take *en route* to equilibrium is not only fundamentally important for emulsion formulations and application (*e.g.* emulsion polymerizations,[26] soft responsive matter,[27,28] enhanced oil recovery[29,30]) but may also provide insight into non-equilibrium

[a] *Department of Chemistry, The Pennsylvania State University, 376 Science Drive, University Park, PA 16802, USA. E-mail: ldz4@psu.edu, spb6056@psu.edu, svk6277@psu.edu, asen@psu.edu*
[b] *Advanced Materials Laboratory, Sandia National Laboratories, 1001 University Blvd SE Ste 100, Albuquerque, NM 87185, USA. E-mail: bjkaehr@sandia.gov*
[c] *Department of Chemical Engineering, The Pennsylvania State University, 121 Chemical and Biomedical Engineering Building, University Park, PA 16802, USA*
[d] *Department of Materials Science and Engineering, The Pennsylvania State University, Steidle Building, University Park, PA 16802, USA*
[e] *Materials Research Institute, The Pennsylvania State University, Millennium Science Complex, University Park, PA 16802, USA*

properties of droplets in other contexts, such as biomolecular condensates.[31] Here, we investigate a phenomenon, and the factors affecting it, wherein solubilizing microscale oil droplets exhibit a significant interfacial instability and dissociate, visually akin to an "explosion" or cellular biological processes such as blebbing and apoptosis.[32]

As emulsion droplets proceed toward equilibrium, they most often remain spherical as governed by surface tension but change diameter over time because of processes like coalescence, ripening, or solubilization. However, under certain conditions, droplets can transition away from sphericity and undergo various non-equilibrium instabilities. For example, droplet interfacial instabilities have been reported prior in droplets composed of highly water-insoluble oils stabilized with hydrophobic, low-HLB (hydrophilic–lipophilic balance) nonionic surfactants. The surfactant transfers into the oil, but solubilization of the oil into the aqueous micelles is negligible.[33–35] Such droplets can evolve protruding myelin-like structures due to the formation of viscous and/or liquid crystalline phases at the interface and in the aqueous phase. Certain zwitterionic surfactants (*e.g.* tetradecyldimethylamine oxide), can elicit similar behavior from hydrocarbon droplets containing alcohols like *n*-heptanol.[36] Recently, our group studied the partitioning of water-miscible nonionic surfactants into oil droplets under a very different set of conditions:[24] oil solubilization into water was significant, and the droplet disappeared at equilibrium to leave behind a single phase. We found that the oil droplets can transiently accumulate high surfactant concentrations (many weight percent), but due to droplet solubilization, that surfactant is released back into the water over time. This overall process generates otherwise unexpected surfactant concentration gradients, the formation of new phases near the drop interface, and drop deformation.[24] Thus, when micellar solubilization and surfactant partitioning are both occurring, the kinetic interplay between these processes may make droplet properties difficult to predict based on equilibrium phase data, like a partition coefficient.

In this work, we characterize the dynamic dissociation behavior of oil emulsion drops in solutions of common nonionic surfactants under conditions of strong oil solubilization into water and surfactant partitioning into oil. These droplets are visually characterized by interfaces that exhibit vanishing interfacial tension, deformation, interfacial fluctuations, and eventually total dissipation into the water phase. We examine the droplet physical properties over time and find that longer alkyl chain oils dissociate at longer times and smaller sizes. We also find that oils with shorter alkyl chains and surfactants with shorter ethylene oxide chains have a greater tendency to dissociate. Counterintuitively, increasing the surfactant concentration favors dissociation only up to a point, beyond which droplets remain spherical and slowly shrink in diameter. Proximity to neighbor droplets suppresses dissociation. We propose a mechanism based on phase inversion that reconciles the observed trends in behavior using the concepts of hydrophilic–lipophilic difference and the separation of different fractions of polydisperse nonionic surfactants through droplet partitioning. Understanding the complex consequences of non-equilibrium partitioning in emulsion droplets can provide fundamental insight into the properties of droplets in diverse contexts such as emulsion polymerizations, active matter, and cellular condensates.

Materials and methods

Chemicals

Oils. 1-Bromopropane purchased from Beantown Chemical (99%), 1-bromobutane purchased from Acros Organics (99%), 1-bromopentane purchased from Alfa Aesar (99%), 1-bromohexane purchased from Alfa Aesar (99%).

Surfactants. Tergitol NP-6, Tergitol NP-9, Tergitol NP-12, Tergitol NP-15, Tergitol NP-30 were purchased from Dow.

Other. Nile Red dye purchased from Chem-Impex International, Inc., 18.2 MΩ ultrapure water was used for surfactant solutions. Cyclohexane was used for surfactant separation. Ammonium hydroxide and glacial acetic acid (99%) purchased from Millipore Sigma were used to make the eluent for liquid chromatography-mass spectrometry.

Experimental methods

Droplet fabrication

Droplets were emulsified by adding 20 μL of oil to 1 mL of water with the desired concentration of surfactant already dissolved, then shaking by hand for a few seconds to produce droplets of a distribution of sizes that contain some droplets the desired target size. In general, the distribution of droplet diameters produced by this method ranges from submicron to hundred μm scale.

Single droplet selection

If a single droplet was required in isolation, as for quantitative analysis of dissociation timing and droplet diameter, then a single droplet from a collection in a dish was extracted in a 1 μL aliquot using a micropipette. The droplet was then added to a second dish with 1 mL of the same surfactant solution for imaging by one of the methods described below.

Droplet cluster containment

The confinement of droplets within a small circular corral was accomplished by pipetting a collection of droplets directly into microfabricated polymer well on a glass coverslip made using multiphoton lithography (Nanoscribe Quantum X). The well had a depth of 400 μm and a radius of 500 μm and was centered within a square region of printed polymer with the coverslip glass serving as the floor of the well (see Fig. S1). Silanization of the coverslip (3-(trimethoxysilyl)propyl methacrylate) and design considerations were employed to facilitate structure adhesion for long term experiments.

Timing procedure

The timing of droplet dissociation was measured using a stopwatch application, taking the start time as the time when the emulsion was fabricated by hand shaking. 1–3 minutes passed between fabrication and microscopic visualization, leading to a difference of no more than a few microns in the diameter between these two timepoints.

Bright-field optical microscopy of droplets

For screening experiments to observe whether dissociation occurred, approximately 20 μL of the emulsion containing just a few droplets was added to 1 mL of the surfactant solution in a small, glass-bottomed, steel dish, which was placed under a Nikon inverted optical microscope adjusted for proper Köhler illumination and examined using bright field microscopy to observe solubilization and dissociation. For experiments requiring a single droplet, imaging was performed after transferring one droplet from this initial droplet mixture to a separate dish by the method described above. The size of the transferred droplet was controlled during this selection and transfer process, rather than initial fabrication, as the simple method of emulsification by hand shaking produced a wide range of drop diameters, from ∼1–200 μm.

Differential interference contrast microscopy of droplets

For some experiments, contrast enhancement by differential interference contrast was used to complement bright-field observation. In this method, a pair of Nomarski prisms, a polarizer with a slight bias angle introduced, and an analyzer (lower polarizer) are used to obtain an image that enhances the contrast from edges and irregularities in samples.

Side-view optical microscopy of droplets

A single droplet was selected by the method described above and added to a glass cuvette containing 1 mL of the desired surfactant solution. The droplet was then observed over time using a custom microscope having a 10× objective oriented perpendicular to the cuvette sidewall and a Basler Ace acA2040 – 55uc camera.

Fluorescence microscopy of droplets

Nile Red dye was dissolved in an aliquot of oil prior to droplet fabrication, which was performed as indicated above with the dye-containing oil. A single droplet was obtained by the method above and imaged in a glass-bottomed, steel dish. After placing the sample on the stage of a Zeiss Axio Observer inverted widefield fluorescence microscope, the droplet was located using brightfield. With a Colibri 7 light source and filters suitable for Nile Red, the droplet was then observed, and a time series was recorded, making sure that the exposure time was long enough that it would remain distinguishable even as the concentration of Nile Red in the droplet diminished due to solubilization. Zeiss Filter Set 91 HE LED, which we used, is a multiband filter set that includes excitation bandpass filters between 406–440, 494–528, and 583–600 nm, beam splitters at 450, 538, and 610 nm, and emission bandpass filters between 458–474, 546–564, and 618–756 nm.

Image analysis

Image and video analysis was carried out using the ImageJ software package. Videos were prepared for publication using Adobe Premiere Pro.

Surfactant separation

30 mL of deionized water and 30 mL of cyclohexane was used to separate more and less polar fractions from 3 g of Tergitol NP-9 in a glass separatory funnel.

Mass spectrometry

Mass spectra of Tergitol surfactants were obtained using a Shimadzu liquid chromatograph and mass spectrograph. Samples of surfactant were dissolved in deionized water at 0.05 wt% (0.5 mg g^{-1}) for analysis, and the eluent used was deionized water with 0.1 wt% NH_4OH and 0.1 wt% acetic acid. The positive ion scan was used to obtain the spectra.

Results and discussion

We began by exploring the non-equilibrium properties of 1-bromo-*n*-alkane micro-droplets dispersed in aqueous solutions of Tergitol NP series surfactants, which are alkylphenol ethoxylates. Brominated alkanes were chosen because they are denser than water which is experimentally convenient. Isolated droplets of 1-bromobutane in 1.0 wt% Tergitol NP-12 (critical micelle concentration, CMC = 0.0085 wt%, hydrophilic lipophilic balance, HLB = 13.8) were placed in a glass-bottomed dish and imaged over time in an optical microscope (Fig. 1A). Droplets of starting diameter 20–200 μm steadily solubilized while remaining nearly spherical, diminishing in size as oil transferred to the water and to surfactant micelles (Fig. 1B). This solubilization behavior was expected, as the shrinkage of droplet diameter over time due to solubilization has been widely studied across a broad range of oils and surfactants.[10,37–41] When we reduced the concentration of Tergitol NP-12 from 1.0 wt% to 0.1 wt%, however, we observed something different: the bromobutane droplet eventually began to exhibit instability, the interface transitioned from smooth to irregular with fluctuating protrusions, water-rich pockets formed in the droplet, and the droplet recovered a spheroidal shape before eventually dissipating into the surrounding solution (Fig. 1C). While we did not expect this behavior in general, we especially would not have expected the droplet to dissociate in this manner exclusively at a *lower* surfactant concentration. Such interfacial instability, which is coupled to lowered interfacial tensions,[24,42] would seem to be more likely with higher surfactant concentrations. This deviation from prototypical solubilization behavior, as well as the intriguing appearance of these droplets, led us to investigate further.

To understand which conditions preferentially give rise to the dissociation behavior, we systematically observed solubilizing micro-droplets composed of a range of 1-bromoalkane oils

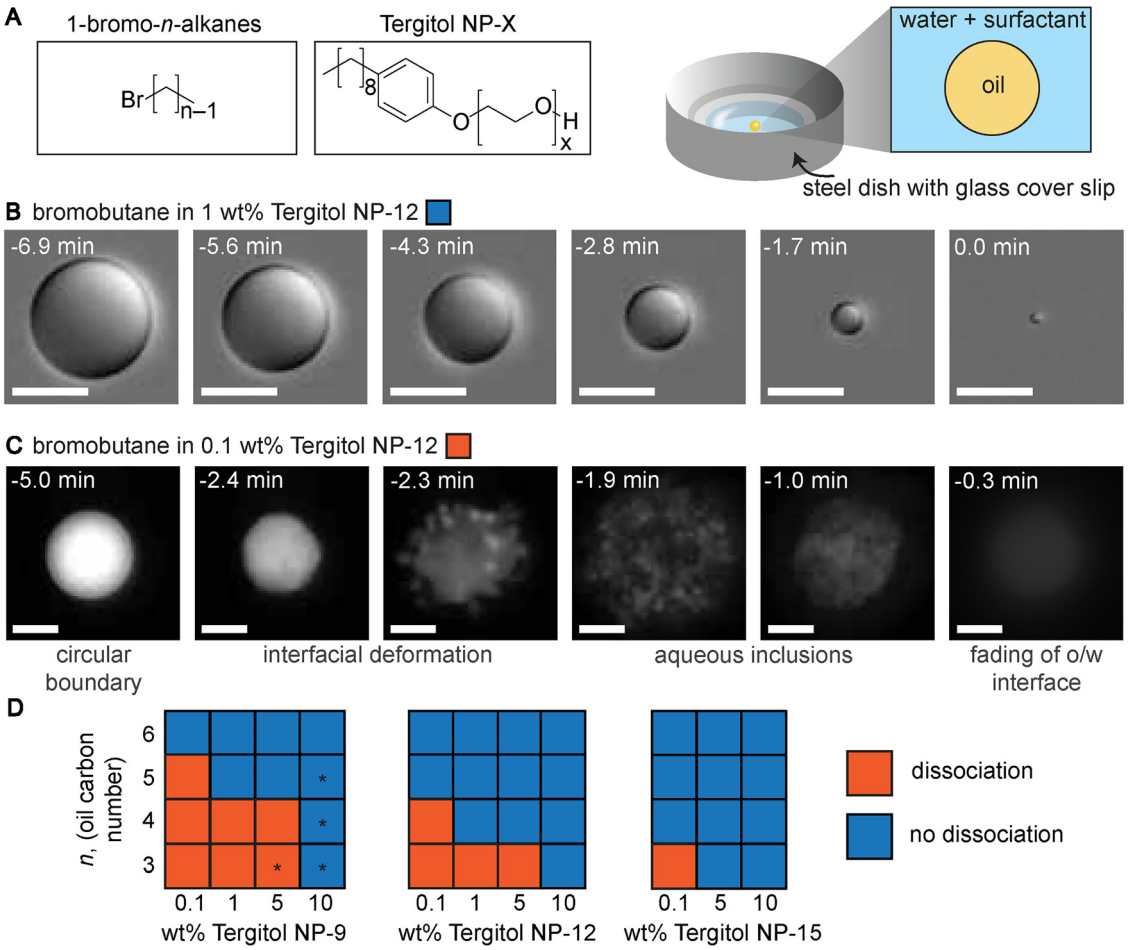

Fig. 1 Dissociation of bromoalkane droplets depends on oil alkyl chain length, surfactant concentration and ethylene oxide number. (A) Chemical structures of the oils and surfactants used and a schematic of the experimental setup. (B) Time-series DIC optical micrographs of a bromobutane droplet solubilizing in 1 wt% Tergitol NP-12. Scale = 25 μm. See Video S1. See Video S2 for fluorescence video with same conditions. (C) Time-series fluorescence micrographs of a bromobutane droplet in 0.1 wt% Tergitol NP-12 that exhibits instability, interfacial deformation, and dissipation behavior. Nile Red dye was added to the oil for fluorescence visualization and the exposure conditions and contrast were kept constant over the time series. Scale = 10 μm. See Video S3. See Video S4 for DIC video with bromobutane droplet in 0.1 wt% Tergitol NP-12. (D) The solubilization of droplets of initial diameter ~20–200 μm with varying bromoalkane oil, surfactant, and surfactant concentration was visually observed and characterized as either undergoing "dissociation" or "no dissociation". The oil is described by carbon number (*n*), surfactant concentration varied between 0.1 and 10 wt%. For each category, at least 5 droplets were analyzed, with a starting diameter falling across the stated range. See Fig. S2 for time-series micrographs of an oil/surfactant pair other than bromobutane and Tergitol NP-12. The asterisks (*) indicate combinations that also result in the formation of a visibly distinct phase surrounding the droplet. See Fig. S3 and Video S5 for details on these (*) cases. HLB: Tergitol NP-9 is 12.9, Tergitol NP-12 is 13.8, Tergitol NP-15 is 15. CMC: Tergitol NP-9 is 0.0060 wt%, Tergitol NP-12 is 0.0085 wt%, Tergitol NP-15 is 0.0090 wt% according to the manufacturer.

(bromopropane, bromobutane, bromopentane, and bromohexane) emulsified by a few seconds of manual shaking in solutions of Tergitol NP-X surfactants (X = 9, 12, 15, referring to the average number of ethylene oxide repeats in the headgroup, EON). Chemical structures are shown in Fig. 1A. In addition to varying the oil and surfactant identity, we tested surfactant concentrations of 0.1 wt%, 1.0 wt%, 5.0 wt%, and 10.0 wt%. For each combination of these conditions, we used brightfield and differential interference contrast (DIC) optical microscopy to observe droplets of varying initial diameters (~20–200 μm). Droplets were kept at very low number density, with just a few droplets in the 1 mL imaging chamber at once, to prevent the influence of droplet neighbors. The behavior of each droplet over the course of its lifetime was categorized either as "dissociation" (*i.e.* interfacial instability led to the rapid dissipation of the droplet as pictured in Fig. 1C) or "no dissociation" (*i.e.* the droplet remained spherical, and the diameter continued to steadily shrink over time until the droplet was no longer clearly visible as pictured in Fig. 1B). In both dissociating and non-dissociating droplets, submicron sized droplets were frequently observed to form inside the main droplet, likely composed of water and surfactant that transfer into the oil over time. The results are shown in Fig. 1D.

Several trends were observed in Fig. 1D. Oils with shorter chain lengths (lower *n*) produced dissociation preferentially over longer chain lengths. For instance, 1-bromohexane never dissociated under the conditions sampled, while bromopropane dissociated under many. Lower EON (also lower HLB)

promoted dissociation, while higher EON suppressed it. For example, bromopentane dissociated in 0.1 wt% Tergitol NP-9 but not in 0.1 wt% Tergitol NP-12, and bromobutane droplets dissociated in 0.1 wt% Tergitol NP-9 and Tergitol NP-12 but not in 0.1 wt% Tergitol NP-15. The concentration of the surfactant in the aqueous phase, C_W, also mattered. Higher C_W suppressed dissociation, while lower C_W favored it. For example, as discussed earlier, a droplet of bromobutane in 0.1 wt% Tergitol NP-12 dissociated, while in 1.0 wt% it did not. In summary, the dissociation behavior was found preferentially for less hydrophobic oils, lower C_W, and smaller surfactant headgroups. Considering what these trends might reveal, we wondered if surfactant partitioning into the droplet could play a role. While the surfactants used are all fully water-miscible, they are also all miscible with all the oils, as tested with a one-to-one mass ratio. We recently reported[24] that solubilizing oil droplets of compositions similar to those used here can uptake nonionic Tergitol surfactants to reach orders-of-magnitude higher concentration in the drop than exists in the water. Thus, we know that these bromoalkane droplets are absorbing surfactant. Some factors that favor dissociation (lower surfactant EON, and less hydrophobic oils) also favor the partitioning of surfactant into the oil,[43] which could indicate that surfactant partitioning into the oil is somehow related. However, we also know that higher C_W leads to a higher surfactant concentration in the oil droplet,[24] and yet we find here that higher C_W actually disfavors dissociation. So, if surfactant partitioning does play a role, dissociation cannot simply be a consequence of reaching some critical concentration of surfactant in the droplet. There must be some other factor(s) at play.

We aimed to uncover more mechanistic insight into what other physical parameters or interfacial transport processes govern this droplet behavior. To do so, we quantitatively characterized the relationship between droplet initial diameter, time elapsed prior to dissociation, and droplet diameter upon dissociation (Fig. 2A). Time of the dissociation was determined using the visual onset of interfacial instability. Defining droplet diameter upon dissociation was more nuanced, because we noticed that many droplets flattened into an oblate spheroid at longer times making the diameter measured with an inverted transmission optical microscope less reliable (Fig. 2A). Droplet flattening indicates that the droplet experiences a decrease in interfacial tension (γ) over time and that gravity dominates over surface tension, indicative of an increasingly higher Bond (also Eötvös) number.[24,25] Although it is known that the Marangoni effect, which does occur in many of our droplets, can give rise to a flattening effect under special circumstances (such as when one liquid becomes wetted to a surface or other liquid phase),[44] we do not believe that the Marangoni effect is playing a significant role in this drop deformation; wetting doesn't usually occur and the Marangoni flow based on tracer particle observations is slight, particularly near the point of dissociation, so likely gravity coupled with low interfacial tension is the main cause of the drop deformation. This observation of droplet flattening and lowered γ has been previously reported by our group to occur in oil droplets of similar size and composition that uptake (partition) surfactant.[24,25] To ensure that the diameter we measured was reasonably reflective of the volume of the droplet, we wanted to find a point near to dissociation that was consistently identifiable by inverted transmission optical microscopy. Since the onset of flattening was gradual, the most distinctive point was when the droplet diameter (D) stopped decreasing because flattening overcame solubilization (*e.g.* when $dD/dt = 0$). Because the droplet

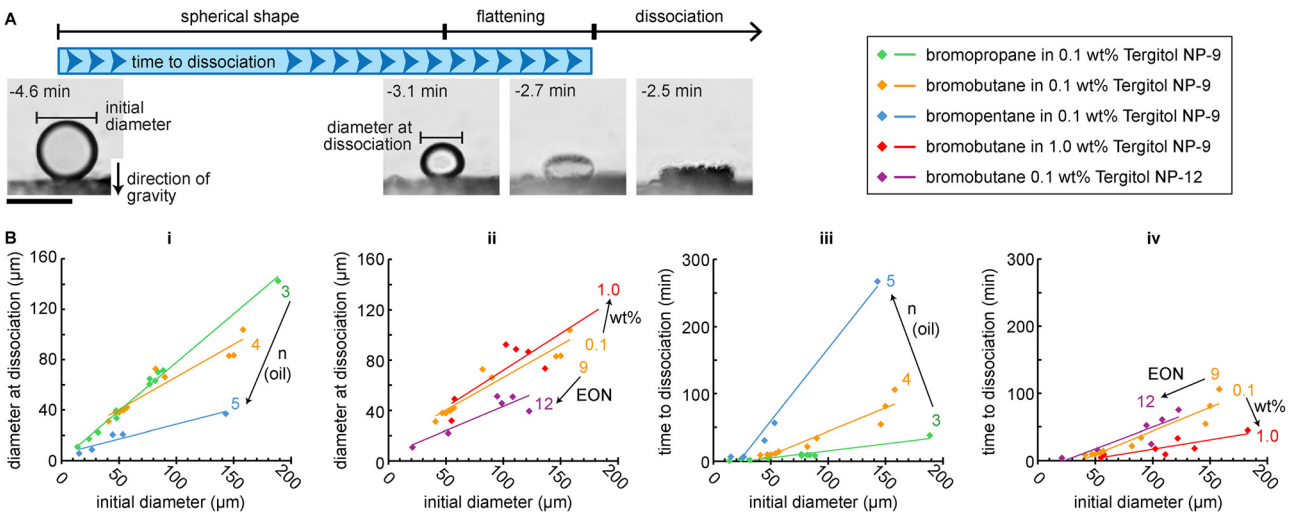

Fig. 2 Quantitative analysis of dissociation timing and drop diameter collected from single droplet experiments. (A) Time-points and measured diameters leading up to droplet dissociation: the initial diameter, the diameter at dissociation (measured with inverted transmission optical microscopy as the point at which the droplet exhibits $dD/dt = 0$). See Fig. S4 for more details on how this point was determined. Below the timeline are side-view micrographs of a bromobutane droplet sitting on the bottom of a cuvette of 0.1 wt% Tergitol NP-9 to illustrate how droplet shape is impacted prior to dissociation and what the initiation of dissociation looks like. Scale = 50 μm. See Fig. S5 for full-size time-series micrographs. (B) Plots of the diameter at dissociation and time to dissociation for selected isolated-droplet systems. (i) and (ii) Diameter at dissociation increases with increasing initial droplet diameter. (iii) and (iv) Time to dissociation increases with initial droplet diameter. Each data point represents one experiment. Linear fit lines are drawn.

generally solubilized faster than it flattened for most of its lifetime, except for the very largest droplets, this point was quite close in time to the dissociation point itself. See Fig. S4 for more details on this method.

Using these approaches to collect time and diameter data, we observed freshly-prepared, isolated droplets with a range of initial diameters between 10 μm and 200 μm and recorded both time to dissociation and diameter at flattening/dissociation, which are plotted in Fig. 2B. There was notable scatter in some of these data sets, which may be related to different flow conditions around droplets of different sizes; Marangoni flow frequently occurred, and Péclet number varies with droplet size and chemical composition.[14] However, there were still some clear trends.

In general, we found that droplets with larger initial diameter dissociated after longer times but at larger diameters than droplets of smaller initial diameter, for constant chemical conditions (Fig. 2B). That is, there is not a ''critical'' diameter or time to be reached. We also noticed that oil droplets of lower carbon number, n, dissociated after shorter times and at larger diameters, compared with the longer-chain oils under the same surfactant and initial diameter conditions (Fig. 2B-i and iii). Again, this is consistent with an influence of surfactant partitioning, since higher concentration of surfactant would be reached faster inside less hydrophobic oils.[24] When the average EON was increased from 9 to 12 (*i.e.* Tergitol NP-9 to NP-12) for bromobutane drops, all else constant, droplets dissociated at smaller sizes (Fig. 2B-ii), and time to dissociation did not change much at a concentration of 0.1 wt% (Fig. 2B-iv). (Note that Tergitol surfactants are polydisperse in EON as reported by the manufacturer, and that the lower EON surfactant molecules are more hydrophobic and thus preferentially partition into the oil over longer EON).[24,43,45] Tergitol NP-9 would thus be a richer source of lower EON molecules than Tergitol NP-12, which seems to favor dissociation, and again could signal a role of surfactant partitioning. When the concentration of Tergitol NP-9 increased from 0.1 wt% to 1 wt% for bromobutane, the effects on diameter at dissociation were small (Fig. 2B-ii), but the time to dissociation was significantly shorter (Fig. 2B-iv).

The relationships between the diameter and time suggest that something about the kinetics of transport of surfactant into and out of the droplet (and higher concentrations of surfactant reached in the droplet[24]) favored dissociation. A revealing observation is that the timescale for reaching the dissociation point can be long (hundreds of minutes). We know from our prior work studying the kinetics of surfactant partitioning into droplets[24] that it only takes on the order of ten to twenty minutes for the surfactant concentration in a microscale drop (radius 100 μm) to plateau to a steady state. Solubilization itself is, however, much slower (hours timescale) which is more similar to the dissociation timescale. This timescale comparison signals that solubilization, which facilitates the transport of oil (and accumulated surfactant) out of the droplet, could be important to the dissociation event.

Based on the quantitative relationships elucidated, our visual observations of the droplet instability, and the inability of previously published mechanisms to adequately explain these results,[36,46,47] we adopted a different hypothesis. We propose here that the droplet dissociation is a result of significant changes in the surfactant concentration and, importantly, molecular weight distribution near the drop interface that forms due to the interplay between surfactant partitioning and solubilization. These changes, particularly in the molecular weight distribution, lead to phase-inversion-like conditions being reached locally near the drop surface; essentially, the composition of surfactant at the interface is altered over time such that is would be preferable to stabilize water-in-oil drops, rather than oil-in-water, leading to instability. Phase inversion refers to the interconversion between an oil-in-water emulsion and a water-in-oil emulsion, which can occur due to changes in phase volume (catastrophic phase inversion) or in variables that alter the characteristic curvature, such as temperature or surfactant compositions (transitional phase inversion).[48] Transitional phase inversions have been studied extensively in oil and water mixtures with nonionic surfactants,[49–52] although these studies necessarily examined dense collections of droplets with more similar oil and water volumes, unlike our isolated droplets. Our droplets do not accomplish a complete phase inversion, but rather a truncated one in which the oil droplet interface destabilizes and disappears due to the small quantity of oil relative to aqueous surfactant, which is below the solubilization capacity of the micelles.

Models have been used to predict and explain how various chemical and physical factors influence transitions between oil-in-water or water-in-oil emulsions. It was first noted by Salager *et al.*[53] that several variables (such as oil chain length, temperature, salinity) are related to the point at which transitional phase inversion occurs. Later, they developed the hydrophilic–lipophilic difference (HLD), a semi-empirical metric akin to HLB, combining several variables to help describe the tendency of a surfactant-oil–water system to form oil-in-water emulsions or water-in-oil emulsions or undergo phase inversion. HLD incorporates the characteristic curvature of the surfactant (a surfactant-specific parameter related to the surfactant's shape), the effect of cosurfactants, the equivalent alkane carbon number (EACN, the ''oiliness'' of the oil), the salinity, and temperature. Simplified by considering zero salinity, no cosurfactant, and constant temperature, the relationship is described by:[54]

$$\mathrm{HLD} = -K \times \mathrm{EACN} + C_c \quad (1)$$

where K is a positive empirical proportionality constant, and C_c is the characteristic curvature of the nonionic surfactant. C_c (also sometimes called σ) relates to the surfactant structure by $C_c = \alpha - \mathrm{EON}$, α being an empirical parameter representing the structure of the tail. So, for the mixture of surfactant molecules considered here, C_c is an average, just as EON is an average. If the average EON at the interface changes, so will the C_c. Oil-in-water emulsions are favored for negative HLD, water-in-oil emulsions are favored for positive HLD, and the inversion process can occur by passing through HLD = 0 (Fig. 3), such as by altering EACN or C_c over time.

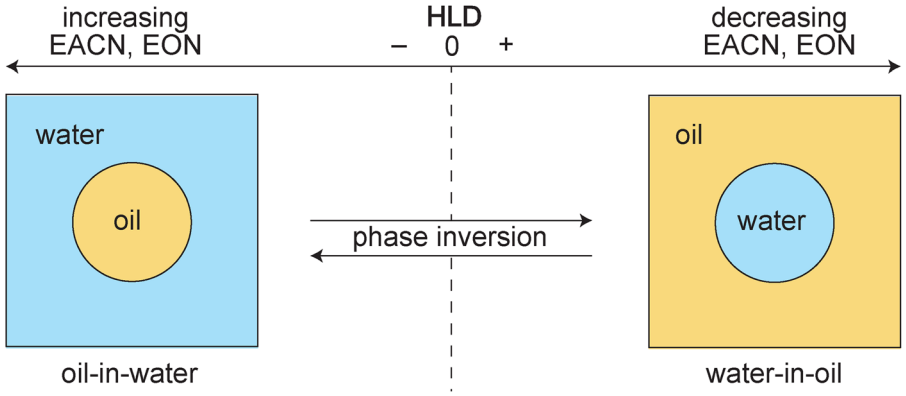

Fig. 3 Schematic depiction of hydrophilic–lipophilic difference and phase inversion. General relationship between the EACN, EON, HLD, and the type of emulsion formed. Specific to this work, Tergitol NP-9, with its average EON of 9, stabilize oil-in-water with a negative HLD, whereas Tergitol NP-6, with an average EON of 6, would stabilize water-in-oil with a positive HLD. Changing the emulsion formulation, such as changing the EON, could lead to transition between positive and negative HLD and induce a transitional phase inversion-like process.

Considering the experimental results and the HLD framework, we propose that temporal changes in the chemical composition of the droplet due to surfactant partitioning (reduction in EACN), and changes in the local environment of the droplet due to solubilization of oil and surfactant (increase in C_c), is leading to conditions that would favor a phase inversion. Fig. 4A provides a schematic guide to the proposed process. Initially, the droplet is composed of pure oil dispersed in aqueous surfactant with concentration C_W; the average surfactant EON near the drop interface, EON_{int}^{avg} is equivalent to the bulk water, EON_W^{avg} (Fig. 4B-i).[24] From our prior work, we know that over a timescale of minutes, surfactant molecules partition into the oil drop and eventually reach a steady state surfactant concentration, C_O^{ss} which can be orders of magnitude higher than in the water, C_W.[24] Surfactant with lower EON (more hydrophobic) partition into oil preferentially (Fig. 4B-ii),[24,43,55] such that the average EON in the oil drop is lower than bulk water, $EON_O^{avg} < EON_W^{avg}$ (Fig. 4B-iii). Surfactant partitioning also lowers the droplet's EACN, raising HLD, since the surfactant molecules are still more polar than the oil. Over time, solubilization removes oil from the droplet, forcing partitioned surfactant to be released back into the water, and we have described this non-equilibrium process in detail in prior work.[24] Accordingly, the interfacial region now becomes a mixture of the surfactant that originates from the water and the oil drop, $EON_O^{avg} < EON_{int}^{avg} < EON_W^{avg}$ (Fig. 4B-iii). Phase inversion is triggered upon reaching a critical interfacial composition that reduces the HLD to zero (Fig. 4B-iv), and this composition would depend upon the specific oil and surfactant. The synergy between these two processes – partitioning of surfactant into the oil droplet followed by solubilization-driven release back into the interfacial region – ultimately can lead to a spontaneous phase inversion which appears as the dissociation of the droplet into the continuous phase. The specific kinetics of the partitioning and solubilization and how the precise distributions of chemicals change over time and space are difficult to measure and model. Convection is also occurring (both from any Marangoni flow occurring at droplet interfaces and from slower thermal convective flows throughout the observation chamber which cannot be completely prevented), so assuming diffusion limitations may not be reasonable. Future work will focus on a full elucidation of this process, while here we focus on the conceptual description.

This conceptual mechanism is particularly helpful in that it can explain our counterintuitive observation that increasing C_W induced dissociation faster (Fig. 2B), but above a certain C_W, droplets never dissociated and rather remained spherical and simply shrank in diameter (Fig. 1). Why can we not simply keep increasing C_W indefinitely and make the dissociation nearly instantaneous? We believe the answer lies in how the composition of the aqueous phase near the drop interface changes over time for different C_W. As C_W increases, the influence of the lower-EON surfactant released from the droplet into the interfacial region – which is responsible for the phase inversion – will decline. In other words, at high C_W, EON_{int}^{avg} is more similar to EON_W^{avg} (*i.e.* no dissociation expected), while at lower C_W, EON_{int}^{avg} is more similar to EON_O^{avg} (dissociation expected) (Fig. 4C).

If the impact of released surfactant on EON_{int}^{avg} is critical to dissociation as we have just described, then the presence of low-EON surfactant is not the only requirement, and adding higher-EON surfactant should suppress dissociation in cases that normally dissociate readily. To test this, we emulsified bromobutane droplets with mixtures of Tergitol NP-9 and Tergitol NP-30. Bromobutane droplets dissociate readily between 0.1 wt% and 5 wt% Tergitol NP-9 (Fig. 1D). With 0.1 wt% Tergitol NP-9 and 0.1 wt% Tergitol NP-30 in the aqueous phase, we still expected EON_{int}^{avg} to be sensitive to low-EON surfactant release, and indeed droplets still dissociated. However, with 1 wt% Tergitol NP-9 and 1 wt% Tergitol NP-30, dissociation no longer occurred, indicating that this significant background concentration of high-EON surfactant prevented the EON_{int}^{avg} from reaching a phase inversion condition. Furthermore, we performed a control experiment removing low-EON surfactant from Tergitol NP-9 using a simple aqueous-cyclohexane separation (mass spectrographs

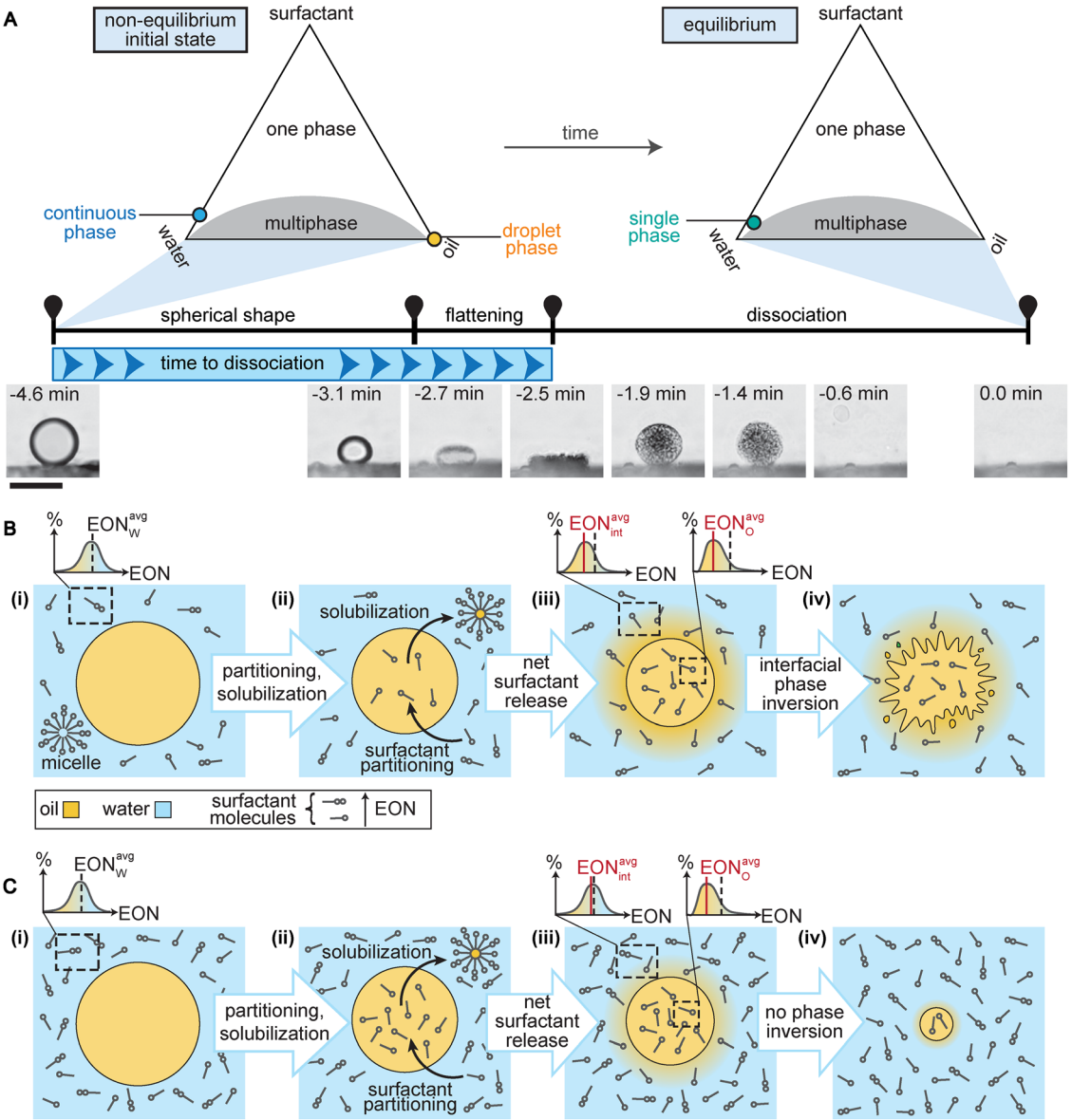

Fig. 4 Proposed mechanism of dissociation where partitioning of predominantly low-EON surfactant molecules leads to local phase inversion conditions during solubilization. (A) Initial non-equilibrium and final equilibrium states of an isolated droplet are depicted using a schematic ternary phase diagram (treating the polydisperse surfactant as a single component), along with a timeline. The droplet first solubilizes and remains spherical, then flattens due to an increasing Bond number. Finally, the droplet dissociates. Scale = 50 μm. (B) The dissociation proceeds by a mechanism involving local HLD conditions triggering phase inversion. (i) An oil droplet begins with no surfactant inside, and with a uniform distribution of surfactant EON everywhere in the continuous phase as shown in the inset plot. (ii) The droplet undergoes simultaneous solubilization and surfactant partitioning, leading to (iii) an enrichment of low-EON surfactant inside the droplet and also outside the droplet. The inset plots show how the average EON (red) has shifted away from the global average (grey) at the interface and inside the droplet. (iv) The resulting low-HLD environment leads to phase inversion conditions near the droplet interface. (C) The non-dissociating droplets proceed similarly to (B) but never achieve a low enough HLD in the interfacial region. This could be for multiple reasons as discussed in the text, but here we draw the more interesting case of an increased C_W as compared to (B). (i,ii) An oil droplet in higher C_W with the same original average EON (inset plot) partitions surfactant and undergoes solubilization, leading to enrichment of low-EON surfactant inside the drop and near the interface over time. (iii) Because of the high C_W, the amount of low-EON surfactant released by a single droplet is not able to modify the average EON in the interfacial region substantially and does not induce dissociation. The inset plots show how the average EON at the interface has not shifted as much from the global average. (iv) The droplet continues to shrink in diameter due to solubilization. Note that the schematics are not drawn to scale, and we did not draw surfactant at the oil–water interface for simplicity.

comparing the modified and unmodified Tergitol NP-9 can be found in Fig. S8), which yielded modified cutoffs – for example, a bromobutane droplet in a 5 wt% solution of modified Tergitol did not dissociate as it would with unmodified Tergitol NP-9 (Fig. S9), instead behaving qualitatively like the 10 wt% solution of Tergitol NP-9. Therefore, in addition to the presence of low-EON surfactant, dissociation also depends on the concentration of high-EON surfactant, and it is important to consider

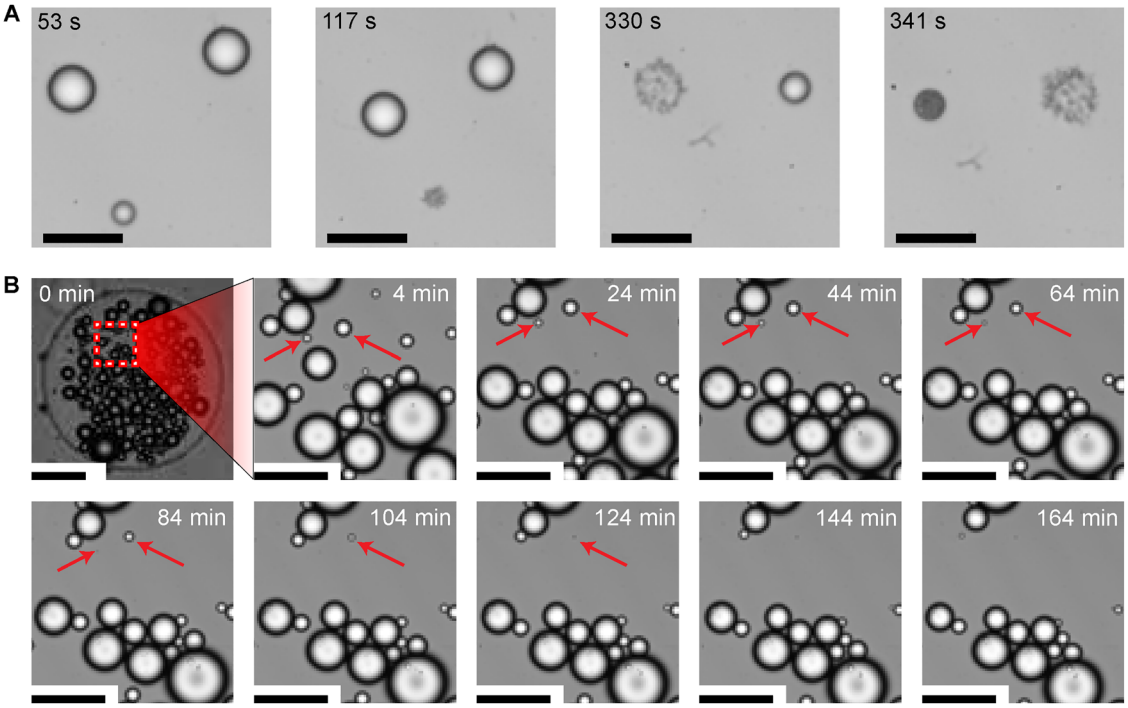

Fig. 5 Solubilization behavior of droplets at high number density diverges from behavior at low number density. (A) A small cluster of bromobutane drops in 0.1 wt% Tergitol NP-9 dissociate, one at a time. Scale = 50 μm. (B) A high number density of bromobutane drops in 0.1 wt% Tergitol NP-9. There are ~170 droplets with diameter >10 μm within a circular well of radius 500 μm within a larger reservoir (1 mL) of surfactant. Drops do not dissociate but rather solubilize and shrink in diameter. Scale = 50 μm, except for first frame, where scale = 250 μm.

how the distribution of EON changes during the non-equilibrium processes.

Because our mechanistic explanation for the dissociation process is related to changes in the distribution of EON, C_W and EON_{int}^{avg}, we expected the dissociation behavior to be influenced by the proximity of neighboring droplets, which can act as sources or sinks of surfactant and release oil and partitioned surfactant *via* solubilization. Our earlier observations used isolated droplets. With more close neighbors, drops compete for access to surfactant, and we also know that droplets solubilize slower as solubilized oil accumulates locally,[39] which agrees with our observations that droplets solubilized very slowly when in the center of dense clusters. Bromobutane droplets in 0.1 wt% Tergitol NP-9, for example, solubilized at $dD/dt \approx 2$–3 μm min^{-1} when isolated but had $dD/dt \approx 0.015$–0.75 μm min^{-1} at various positions in a large droplet cluster. While bromobutane droplets in 1 wt% Tergitol NP-9 in a low-density cluster dissociate readily (Fig. 5A), droplets in a high-density cluster shrink more slowly and often never dissociate (Fig. 5B). Slower solubilization itself, which prevents local accumulation of the low-EON surfactant near the interface, coupled with competition for the partitioning of surfactant across many droplets, are likely to act synergistically to suppress the dissociation process. After a long time, when only a few of the original droplets remain thus creating a low-number-density condition, these remaining droplets dissociate. Dissociation suppression by neighbor droplets speaks to the importance of local environment on the non-equilibrium processes that affect droplet properties and suggests that chemical signaling between droplets can be used to control this type of behavior.

Conclusions

Dynamic behavior of oil–water interfaces has long been recognized as centrally important for understanding and designing interfaces in a wide range of applications, including advanced soft and cell-mimetic materials synthesis,[27,28] enhanced oil recovery,[29,30,56] environmental remediation (such as groundwater contaminant removal),[57] and targeted delivery and controlled release of drug molecules.[58,59] As a result, fundamental research on dynamic activity in droplets and other microscale interfaces has been pursued frequently over the last several decades, including much insightful work on similar kinds of behavior to the present work, from spontaneous emulsification[21,35,60] and optimum detergency[61,62] to diffusion path analysis[21,33,34,63] and phase behavior in oil-surfactant-water systems.[33] These studies have reported many visually interesting phenomena that can be observed, and provided a wealth of data on the type of conditions that can give rise to them, helping to inspire our study.

Microscale liquid phases and interfaces can develop surprising properties and dynamic behavior through micellar solubilization and surfactant partitioning, including the dynamic dissociation behavior of oil emulsion drops that we

characterized here. These dissociating droplets exhibited vanishing interfacial tension, flattening deformation, and developed finger-like protrusions and cavities in their interface before dissipating into the surrounding solution. Measurement of time to reach dissociation and droplet diameter just before dissociation revealed trends including the following: droplets of more hydrophobic oils dissociated at longer times and smaller sizes, droplets in a higher surfactant concentration dissociated earlier and at comparable sizes to droplets at lower concentration, and droplets in higher ethylene oxide number surfactant dissociated at comparable times but smaller sizes than droplets in lower ethylene oxide number surfactant. However, there are limits to all these trends – *e.g.* if the oil is too hydrophobic, there is too high of a surfactant concentration, and too high an ethylene oxide number, no dissociation occurs, signaling a balance of these factors in determining the dissociation process.

We propose a mechanism of localized phase inversion conditions that accounts for our observations. Polydisperse nonionic surfactants partition into bromoalkane oil droplets over short timescales (few minutes), leading the oil phase to be more polar and the droplet-internal surfactant fraction to have a lower average EON than the water phase. Subsequent solubilization of the oil and transfer of the accumulated surfactant back into the water (over tens of minutes/hours timescale) leads to modulation of the droplet's local environment; interfacial tension is reduced and HLD approaches zero, and the droplet destabilizes. This process is dependent upon droplet neighbors, which compete for surfactant and thus have modified solubilization kinetics and partitioning. Our investigation provides perspective for how the kinetics of different transport processes in non-equilibrium droplets can influence droplet temporal properties and why these properties may vary so significantly based on small changes in chemical composition or physical environment. Understanding the interactions between these pathways and their impact on emulsion properties may have impact in areas that rely on far-from-equilibrium multiphase systems, like active emulsions, biomolecular condensates, oil recovery or emulsion polymerization.

Conflicts of interest

The authors declare no conflicts of interest.

Data availability

The data supporting this article have been included as part of the supplementary information (SI). Supplementary information is available. See DOI: https://doi.org/10.1039/d5sm01049g.

Acknowledgements

We thank and acknowledge funding from the Army Research Office (W911NF-18-1-0414), the Alfred P. Sloan Foundation (G-2023-19642) and the Camille and Henry Dreyfus Foundation (TC-22-023). We also thank Alexander C. Castonguay and Yasmarie Colón, whose observations and conversations led to the starting point for this project. Special thanks to Nathaniel Sturniolo, who provided useful knowledge on contrast enhancement techniques that were implemented in our microscopy work. This work was performed, in part, at the Center for Integrated Nanotechnologies, an Office of Science User Facility operated for the U.S. Department of Energy (DOE) Office of Science. Sandia National Laboratories is a multimission laboratory managed and operated by National Technology & Engineering Solutions of Sandia, LLC, a wholly owned subsidiary of Honeywell International, NC., for the U.S. DOE's National Nuclear Security Administration under contract DE-NA-0003525. The views expressed in the article do not necessarily represent the views of the U.S. DOE or the United States Government.

References

1 I. Capek, Degradation of Kinetically-Stable o/w Emulsions, *Adv. Colloid Interface Sci.*, 2004, **107**(2–3), 125–155, DOI: 10.1016/S0001-8686(03)00115-5.
2 A. C. Donegan and A. J. I. Ward, Solubilization Kinetics of N-Alkanes by a Non-Ionic Surfactant, *J. Pharm. Pharmacol.*, 1987, **39**(1), 45–47, DOI: 10.1111/J.2042-7158.1987.TB07160.X.
3 M. J. Rosen, *Surfactants and Interfacial Phenomena*, 3rd edn, Wiley-Interscience, Hoboken, 2004, DOI: 10.1093/jaoac/62.3.700.
4 A. Graciaa, J. Andérez, C. Bracho, J. Lachaise, J. L. Salager, L. Tolosa and F. Ysambertt, The Selective Partitioning of the Oligomers of Polyethoxylated Surfactant Mixtures between Interface and Oil and Water Bulk Phases, *Adv. Colloid Interface Sci.*, 2006, **123–126**, 63–73, DOI: 10.1016/j.cis.2006.05.015.
5 F. Ravera, M. Ferrari, L. Liggieri, R. Miller and A. Passerone, Measurement of the Partition Coefficient of Surfactants in Water/Oil Systems, *Langmuir*, 1997, **13**(18), 4817–4820, DOI: 10.1021/la962096.
6 G. Catanoiu, E. Carey, S. R. Patil, S. Engelskirchen and C. Stubenrauch, Partition Coefficients of Nonionic Surfactants in Water/n-Alkane Systems, *J. Colloid Interface Sci.*, 2011, **355**(1), 150–156, DOI: 10.1016/j.jcis.2010.12.002.
7 J. Weiss and D. J. McClements, Mass Transport Phenomena in Oil-in-Water Emulsions Containing Surfactant Micelles: Solubilization, *Langmuir*, 2000, **16**(14), 5879–5883, DOI: 10.1021/la9914763.
8 H. Manikantan and T. M. Squires, Surfactant Dynamics: Hidden Variables Controlling Fluid Flows, *J. Fluid Mech.*, 2020, 892, DOI: 10.1017/jfm.2020.170.Surfactant.
9 S. Herminghaus, C. C. Maass, C. Krüger, S. Thutupalli, L. Goehring and C. Bahr, Interfacial Mechanisms in Active Emulsions, *Soft Matter*, 2014, **10**(36), 7008–7022, DOI: 10.1039/c4sm00550c.
10 S. R. Dungan, B. H. Tai and N. I. Gerhardt, Transport Mechanisms in the Micellar Solubilization of Alkanes in

Oil-in-Water Emulsions, *Colloids Surf., A*, 2003, **216**(1–3), 149–166, DOI: 10.1016/S0927-7757(02)00549-6.

11 S. Michelin, Self-Propulsion of Chemically Active Droplets, *Annu. Rev. Fluid Mech.*, 2023, **55**, 77–101, DOI: 10.1146/annurev-fluid-120720-012204.

12 C. M. Wentworth, A. C. Castonguay, P. G. Moerman, C. H. Meredith, R. V. Balaj, S. I. Cheon and L. D. Zarzar, Chemically Tuning Attractive and Repulsive Interactions between Solubilizing Oil Droplets, *Angew. Chem., Int. Ed.*, 2022, **61**(32), e202204510, DOI: 10.1002/anie.202204510.

13 S. Birrer, S. I. Cheon and L. D. Zarzar, We the Droplets: A Constitutional Approach to Active and Self-Propelled Emulsions, *Curr. Opin. Colloid Interface Sci.*, 2022, **61**, 101623, DOI: 10.1016/j.cocis.2022.101623.

14 A. A. Peña and C. A. Miller, Solubilization Rates of Oils in Surfactant Solutions and Their Relationship to Mass Transport in Emulsions, *Adv. Colloid Interface Sci.*, 2006, **123–126**, 241–257, DOI: 10.1016/j.cis.2006.05.005.

15 C. C. Maass, C. Krüger, S. Herminghaus and C. Bahr, Swimming Droplets, *Annu. Rev. Condens. Matter Phys.*, 2016, **7**, 171–193, DOI: 10.1146/annurev-conmatphys-031115-011517.

16 P. G. Moerman, H. W. Moyses, E. B. Van Der Wee, D. G. Grier, A. Van Blaaderen, W. K. Kegel, J. Groenewold and J. Brujic, Solute-Mediated Interactions between Active Droplets, *Phys. Rev. E*, 2017, **96**(3), 32607, DOI: 10.1103/PhysRevE.96.032607.

17 C. H. Meredith, P. G. Moerman, J. Groenewold, Y. J. Chiu, W. K. Kegel, A. van Blaaderen and L. D. Zarzar, Predator–Prey Interactions between Droplets Driven by Non-Reciprocal Oil Exchange, *Nat. Chem.*, 2020, **12**(12), 1136–1142, DOI: 10.1038/s41557-020-00575-0.

18 Y. Liu, R. Kailasham, P. G. Moerman, A. S. Khair and L. Zarzar, Self-Organized Patterns in Non-Reciprocal Active Droplet Systems, *Angew. Chem., Int. Ed.*, 2024, e202409382, DOI: 10.1002/anie.202409382.

19 C. Krüger, C. Bahr, S. Herminghaus and C. C. Maass, Dimensionality Matters in the Collective Behaviour of Active Emulsions, *Eur. Phys. J. E*, 2016, **39**(6), 64, DOI: 10.1140/epje/i2016-16064-y.

20 C. Solans, D. Morales and M. Homs, Spontaneous Emulsification, *Curr. Opin. Colloid Interface Sci.*, 2016, **22**, 88–93, DOI: 10.1016/j.cocis.2016.03.002.

21 C. A. Miller, Spontaneous Emulsification Produced by Diffusion - A Review, *Colloids Surf.*, 1988, **29**(1), 89–102, DOI: 10.1016/0166-6622(88)80173-2.

22 N. Shahidzadeh, D. Bonn and J. Meunier, A New Mechanism of Spontaneous Emulsification: Relation to Surfactant Properties, *Europhys. Lett.*, 1997, **40**(4), 459–464.

23 R. Granek, R. C. Ball and M. E. Cates, Dynamics of Spontaneous Emulsification, *J. Phys. II*, 1993, **3**(6), 829–849, DOI: 10.1051/jp2:1993170.

24 R. V. Balaj, W. Xue, P. Bayati, S. Mallory and L. D. Zarzar, Dynamic Partitioning of Surfactants into Nonequilibrium Emulsion Droplets, *J. Am. Chem. Soc.*, 2024, **146**(38), 26340–26350, DOI: 10.1021/jacs.4c08917.

25 K. E. Kim, W. Xue and L. D. Zarzar, Liquid-Liquid Surfactant Partitioning Drives Dewetting of Oil from Hydrophobic Surfaces, *J. Colloid Interface Sci.*, 2024, **658**, 179–187, DOI: 10.1016/j.jcis.2023.12.054.

26 P. A. Lovell and F. J. Schork, Fundamentals of Emulsion Polymerization, *Biomacromolecules*, 2020, **21**(11), 4396–4441, DOI: 10.1021/acs.biomac.0c00769.

27 H. Wang, X. Xiong, L. Yang and J. Cui, Droplets in Soft Materials, *Droplet*, 2022, **1**(2), 110–138, DOI: 10.1002/dro2.24.

28 F. G. Downs, D. J. Lunn, M. J. Booth, J. B. Sauer, W. J. Ramsay, R. G. Klemperer, C. J. Hawker and H. Bayley, Multi-Responsive Hydrogel Structures from Patterned Droplet Networks, *Nat. Chem.*, 2020, **12**(4), 363–371, DOI: 10.1038/s41557-020-0444-1.

29 T. T. Nguyen, C. Morgan, L. Poindexter and J. Fernandez, Application of the Hydrophilic–Lipophilic Deviation Concept to Surfactant Characterization and Surfactant Selection for Enhanced Oil Recovery, *J. Surfactants Deterg.*, 2019, **22**(5), 983–999, DOI: 10.1002/jsde.12305.

30 W. Chen and D. S. Schechter, Surfactant Selection for Enhanced Oil Recovery Based on Surfactant Molecular Structure in Unconventional Liquid Reservoirs, *J. Pet. Sci. Eng.*, 2021, **196**(2020), 107702, DOI: 10.1016/j.petrol.2020.107702.

31 S. F. Banani, H. O. Lee, A. A. Hyman and M. K. Rosen, Biomolecular Condensates: Organizers of Cellular Biochemistry, *Nat. Rev. Mol. Cell Biol.*, 2017, **18**(5), 285–298, DOI: 10.1038/nrm.2017.7.

32 C. M. Henry, E. Hollville and S. J. Martin, Measuring Apoptosis by Microscopy and Flow Cytometry, *Methods*, 2013, **61**(2), 90–97, DOI: 10.1016/j.ymeth.2013.01.008.

33 W. J. Benton, K. H. Raney and C. A. Miller, Enhanced Videomicroscopy of Phase Transitions and Diffusional Phenomena in Oil-Water-Nonionic Surfactant Systems, *J. Colloid Interface Sci.*, 1986, **110**(2), 363–388, DOI: 10.1016/0021-9797(86)90390-5.

34 J. C. Lim and C. A. Miller, Dynamic Behavior and Detergency in Systems Containing Nonionic Surfactants and Mixtures of Polar and Nonpolar Oils, *Langmuir*, 1991, **7**(10), 2021–2027, DOI: 10.1021/la00058a010.

35 T. Nishimi and C. A. Miller, Spontaneous Emulsification Produced by Chemical Reactions, *J. Colloid Interface Sci.*, 2001, **237**(2), 259–266, DOI: 10.1006/jcis.2001.7467.

36 M. J. Rang, C. A. Miller, H. H. Hoffmann and C. Thunig, Behavior of Hydrocarbon/Alcohol Drops Injected into Dilute Solutions of an Amine Oxide Surfactant, *Ind. Eng. Chem. Res.*, 1996, **35**(9), 3233–3240, DOI: 10.1021/ie960077p.

37 P. D. Todorov, G. S. Marinov, P. A. Kralchevsky, N. D. Denkov, P. Durbut, G. Broze and A. Mehreteab, Kinetics of Triglyceride Solubilization by Micellar Solutions of Nonionic Surfactant and Triblock Copolymer. 3. Experiments with Single Drops, *Langmuir*, 2002, **18**(21), 7896–7905, DOI: 10.1021/LA020367C.

38 P. D. Todorov, P. A. Kralchevsky, N. D. Denkov, G. Broze and A. Mehreteab, Kinetics of Solubilization of N-Decane and

Benzene by Micellar Solutions of Sodium Dodecyl Sulfate, *J. Colloid Interface Sci.*, 2002, **245**(2), 371–382, DOI: 10.1006/JCIS.2001.8031.

39 S. Ariyaprakai and S. R. Dungan, Solubilization in Monodisperse Emulsions, *J. Colloid Interface Sci.*, 2007, **314**(2), 673–682, DOI: 10.1016/j.jcis.2007.06.004.

40 B. J. Carroll, The Kinetics of Solubilization of Nonpolar Oils by Nonionic Surfactant Solutions, *J. Colloid Interface Sci.*, 1981, **79**(1), 126–135, DOI: 10.1016/0021-9797(81)90055-2.

41 B. J. Carroll and P. J. Doyle, Solubilization Kinetics of a Triglyceride/n-Alkane Mixture in a Non-Ionic Surfactant Solution, *J. Pharm. Pharmacol.*, 1988, **40**(4), 229–232, DOI: 10.1111/J.2042-7158.1988.TB05233.X.

42 A. Sauret, C. Spandagos and H. C. Shum, Fluctuation-Induced Dynamics of Multiphase Liquid Jets with Ultra-Low Interfacial Tension, *Lab Chip*, 2012, **12**(18), 3380–3386, DOI: 10.1039/c2lc40524e.

43 G. G. Warr, F. Grieser and T. W. Healy, Distribution of Polydisperse Nonionic Surfactants between Oil and Water, *J. Phys. Chem.*, 1983, **87**(22), 4520–4524, DOI: 10.1021/j100245a036.

44 R. B. J. Koldeweij, B. F. Van Capelleveen, D. Lohse and C. W. Visser, Marangoni-Driven Spreading of Miscible Liquids in the Binary Pendant Drop Geometry, *Soft Matter*, 2019, **15**(42), 8525–8531, DOI: 10.1039/c8sm02074d.

45 E. H. Crook, D. B. Fordyce and G. F. Trebbi, Molecular Weight Distribution of Nonionic Surfactants: II. Partition Coefficients of Normal Distribution and Homogeneous p, t-Octylphenoxyethoxy-Ethanols (OPE's), *J. Colloid Sci.*, 1965, **20**(3), 191–204, DOI: 10.1016/0095-8522(65)90010-3.

46 M. J. Rang, J. C. Lim, C. A. Miller, C. Thunig and H. H. Hoffmann, Dynamic Behavior of Alcohol Drops in Dilute Solutions of an Amine Oxide Surfactant, *J. Colloid Interface Sci.*, 1995, 440–447, DOI: 10.1006/jcis.1995.1474.

47 M. J. Rang and C. A. Miller, Spontaneous Emulsification of Oil Drops Containing Surfactants and Medium-Chain Alcohols, *Prog. Colloid Polym. Sci.*, 1998, **109**, 101–117, DOI: 10.1007/bfb0118162.

48 A. Kumar, S. Li, C. M. Cheng and D. Lee, Recent Developments in Phase Inversion Emulsification, *Ind. Eng. Chem. Res.*, 2015, **54**(34), 8375–8396, DOI: 10.1021/acs.iecr.5b01122.

49 M. Pérez, N. Zambrano, M. Ramirez, E. Tyrode and J. L. Salager, Surfactant-Oil-Water Systems near the Affinity Inversion. XII. Emulsion Drop Size versus Formulation and Composition, *J. Dispers. Sci. Technol.*, 2002, **23**(1–3), 55–63, DOI: 10.1081/DIS-120003304.

50 M. Zerfa, S. Sajjadi and B. W. Brooks, Phase Behaviour of Polymer Emulsions during the Phase Inversion Process in the Presence of Non-Ionic Surfactants, *Colloids Surf., A*, 2001, **178**(1–3), 41–48, DOI: 10.1016/S0927-7757(00)00728-7.

51 S. Sajjadi, M. Zerfa and B. W. Brooks, Phase Inversion in P-Xylene/Water Emulsions with the Non-Ionic Surfactant Pair Sorbitan Monolaurate/Polyoxyethylene Sorbitan Monolaurate (Span 20/Tween 20), *Colloids Surf., A*, 2003, **218**(1–3), 241–254, DOI: 10.1016/S0927-7757(02)00596-4.

52 S. Sajjadi, F. Jahanzad and M. Yianneskis, Catastrophic Phase Inversion of Abnormal Emulsions in the Vicinity of the Locus of Transitional Inversion, *Colloids Surf., A*, 2004, **240**(1–3), 149–155, DOI: 10.1016/j.colsurfa.2004.03.012.

53 J. L. Salager, J. C. Morgan, R. S. Schechter, W. H. Wade and E. Vasquez, Optimum Formulation of Surfactant-Water-Oil Systems for Minimum Interfacial Tension or Phase Behaviour, *Soc. Pet. Eng. J.*, 1979, **19**, 107–115.

54 E. J. Acosta, The HLD-NAC Equation of State for Microemulsions Formulated with Nonionic Alcohol Ethoxylate and Alkylphenol Ethoxylate Surfactants, *Colloids Surf., A*, 2008, **320**(1–3), 193–204, DOI: 10.1016/j.colsurfa.2008.01.049.

55 A. Graciaa, J. Lachaise, M. Bourrel, I. Osborne-Lee, R. E. Schechter and W. H. Wade, Partitioning of Nonionic and Anionic Surfactant Mixtures Between Oil/Microemulsion/Water Phases, *SPE Reserv. Eng.*, 1987, **2**(3), 305–314, DOI: 10.2118/13030-PA.

56 Z. Li, D. Xu, Y. Yuan, H. Wu, J. Hou, W. Kang and B. Bai, Advances of Spontaneous Emulsification and Its Important Applications in Enhanced Oil Recovery Process, *Adv. Colloid Interface Sci.*, 2020, **277**, 102119, DOI: 10.1016/j.cis.2020.102119.

57 E. C. Butler and K. F. Hayes, Micellar Solubilization of Nonaqueous Phase Liquid Contaminants by Nonionic Surfactant Mixtures: Effects of Sorption, Partitioning and Mixing, *Water Res.*, 1998, **32**(5), 1345–1354, DOI: 10.1016/S0043-1354(97)00360-6.

58 A. Perazzo, V. Preziosi and S. Guido, Phase Inversion Emulsification: Current Understanding and Applications, *Adv. Colloid Interface Sci.*, 2015, **222**, 581–599, DOI: 10.1016/j.cis.2015.01.001.

59 R. J. Wilson, Y. Li, G. Yang and C. X. Zhao, Nanoemulsions for Drug Delivery, *Particuology*, 2022, **64**, 85–97, DOI: 10.1016/j.partic.2021.05.009.

60 T. Tungsubutra and C. A. Miller, Effect of Secondary Alcohol Ethoxylates on Behavior of Triolein-Water-Surfactant Systems, *J. Am. Oil Chem. Soc.*, 1994, **71**(1), 65–73, DOI: 10.1007/BF02541474.

61 K. H. Raney and C. A. Miller, Optimum Detergency Conditions with Nonionic Surfactants, *J. Colloid Interface Sci.*, 1987, **119**(2), 539–549, DOI: 10.1016/0021-9797(87)90301-8.

62 L. Thompson, The Role of Oil Detachment Mechanisms in Determining Optimum Detergency Conditions, *J. Colloid Interface Sci.*, 1994, **163**, 61–73.

63 K. J. Ruschak and C. A. Miller, Spontaneous Emulsification in Ternary Systems with Mass Transfer, *Ind. Eng. Chem. Fundam.*, 1972, **11**(4), 534–540, DOI: 10.1021/i160044a017.